ANALYSIS OF THE CENTRAL NERVOUS SYSTEM IN A MOUSE MODEL OF HSAN TYPE III

by

Hannah Rose Waller

A thesis submitted in partial fulfillment
of the requirements for the degree

of

Master of Science

in

Neuroscience

MONTANA STATE UNIVERSITY
Bozeman, Montana

November 2013

APPROVAL

of a thesis submitted by

Hannah Rose Waller

This thesis has been read by each member of the thesis committee and has been found to be satisfactory regarding content, English usage, format, citation, bibliographic style, and consistency and is ready for submission to The Graduate School.

Dr. Frances Lefcort

Approved for the Department of Cellular Biology and Neuroscience

Dr. Frances Lefcort

Approved for the The Graduate School

Dr. Ronald W. Larsen

STATEMENT OF PERMISSION TO USE

In presenting this thesis in partial fulfillment of the requirements for a master's degree at Montana State University, I agree that the Library shall make it available to borrowers under rules of the Library.

If I have indicated my intention to copyright this thesis by including a copyright notice page, copying is allowable only for scholarly purposes, consistent with "fair use" as prescribed in the U.S. Copyright Law. Requests for permission for extended quotation from or reproduction of this thesis in whole or in parts may be granted only by the copyright holder.

Hannah Rose Waller

November 2013

TABLE OF CONTENTS

TABLE OF CONTENTS CONTINUED

LIST OF TABLES

Table Page

LIST OF FIGURES

ABSTRACT

Familial Dysautonomia (FD), also called Riley Day Syndrome, is a Hereditary Sensory and Autonomic Neuropathy (HSAN Type III) that is characterized by dysfunction of the sensory and autonomic nervous systems. The disease is caused by a severe reduction in levels of the protein IKAP as a result of a point mutation in *Ikbkap* mRNA which results in targeting of the mRNA for nonsense mediated decay. In humans, symptoms include autonomic crises, tachycardia, blood pressure lability, lack of overflow tears, decreased pain and temperature sensation, and scoliosis. Half of affected individuals die by age 40.

Although FD has been traditionally classified as a disease of the autonomic nervous system, there have been notable effects observed in the central nervous system (CNS) as well, though many of these observations remain to be quantified. The presented study evaluated the impact of FD on the CNS using a mouse model where *Ikbkap* was deleted selectively from neurons of the CNS. For this model, a conditional knockout (CKO) strategy was employed because mice that are null for *Ikbkap* die by embryonic day 10.5, precluding their usefulness for analyzing FD in the adult CNS. For this study, morphological analyses and immunohistochemical staining were performed on the brain tissue.

Affected mice were found to have a significant reduction in choline acetyltransferase (ChAT) positive neurons in the dorsal motor nucleus of the vagus nerve (DMNX) relative to controls, indicating potential decreased parasympathetic innervation of the nucleus in the heart and other target organs. Additionally, the size of the lateral ventricles and hippocampus relative to hemisphere size was significantly increased for the mutant mice. Further, the corpus callosum and lateral amygdaloid nucleus areas were significantly decreased relative to wild-type controls. Cortical layering was found to be normal in *Tα1tubulin-Cre/Ikbkap* CKO mice. Taken together, these results suggest that the morphological differences are associated with increased cell death and decreased neurogenesis and cell differentiation.

The neural and morphological findings presented in this study are the first data demonstrating perturbations in the CNS of a mouse model for FD and may explain some of the phenotypes observed in FD patients.

CHAPTER ONE

INTRODUCTION

Introduction to Familial Dysautonomia

Familial Dysautonomia (also called Riley Day Syndrome) is a Hereditary Sensory Autonomic Neuropathy Type III (HSAN III) and is most prevalent in the Ashkenazi Jewish population, where one in 30 individuals is a carrier (1). Affected individuals present with a broad spectrum of symptoms including tachycardia, labile blood pressure, autonomic vomiting and syncope crises, scoliosis, and reduced pain and temperature sensation. The disease is a result of mutation in the gene *Ikbkap*, which is located on the long arm of chromosome 9. Mutations cause variable skipping of exon 20, resulting in production of a premature stop codon, and ultimately a reduction in levels of functional inhibitor of kappaB kinase complex associated protein (IKAP). In the majority of patients, position 6 of the donor splice site of intron 20 contains a T to C transition, leading to a frame shift and mutated mRNA which becomes targeted for nonsense mediated decay. While all patients do express wild type *Ikbkap* mRNA, there is consistent, well-established under-expression in tissues of the sensory and autonomic nervous systems. Furthermore, despite the commonality in mutation among patients (seen in over 98 percent of cases), there is wide variability in phenotype and symptom severity. The decreased IKAP levels manifest in the form of Familial Dysautonomia, which is marked by underdevelopment and progressive degeneration of both the sensory and autonomic nervous systems (1).

The nervous system is composed of two branches, the peripheral nervous system (PNS), and the central nervous system (CNS), which includes the brain and spinal cord. The PNS has two further branches, the somatic nervous system, and the autonomic nervous system (ANS), which contains the sympathetic and parasympathetic nervous systems responsible for maintaining homeostasis and for innervating and regulating bodily tissues and organs including cardiac muscle, smooth muscle, and glands (42, 36). Despite the traditional classification of FD as a disease primarily affecting the ANS, there is emerging evidence for effects in the CNS as well. Analysis of the human FD brain using Magnetic Resonance Imaging (MRI) and Diffusion Tensor Imaging (DTI) have identified compromised integrity in both white and gray matter structures in FD brains compared to controls as well as abnormally low white matter to gray matter ratios (26). This is particularly intriguing because one proposed role of IKAP is in the formation of myelin (48). Furthermore, when patients were cerebrally perfused using single photon emission cerebral tomography (SPECT) during dysautonomic crisis, there was hyperperfusion in certain regions of the brain, similar to what would occur during seizure (27). This provides evidence of CNS perturbation in the FD brain. Frequent grand mal seizures, fever, and abnormal electroencephalogram (EEG) are also observed in FD patients (29), indicative of CNS dysfunction. There is already an established function for IKAP in the ANS (1, 10, 28, 43) but its role in the CNS remains less clear. In efforts to elucidate this role, a conditional knockout mouse model of FD was generated for the present series of experiments. For this model, *Ikbkap* was knocked out of cells only in the CNS containing alpha-tubulin, a constituent of microtubules in neurons. This conditional

knockout strategy was necessary because mice that are completely null for *Ikbkap* die by embryonic day 10.5. Since the goal of this study was to examine the effects of FD in the fully developed mouse CNS, this approach allowed for analysis in adult mice. The brain morphology of these mutant mice was then analyzed and compared to littermate controls in the present study.

Introduction to Elongator Complex

IKAP is also referred to as Elp1, and is a subunit of the RNA Polymerase II Elongator complex, which has a multitude of distinct proposed functions (3). Initially postulated to assist the transcription complex through its role of acetylating nucleosomes, subsequent research suggested that the Elongator complex plays a cellular role in both the nucleus and cytoplasm (49). Research has indicated a role for Elongator in cytoskeleton organization, c-Jun N terminal Kinase (JNK) mediated stress signaling and other apoptosis regulation, exocytosis, and in tRNA modification (3, 49, 50). Furthermore, recent evidence suggests that decreasing levels of *Ikbkap* mRNA delays the migration of neurons in the cerebral cortex during development (3). This may be a result of destabilization of the subunit Elp3, which results in decreased acetylation of microtubules in the cell, thereby resulting in defects in neural migration and dendritic branching during development. Since patients of FD may display lower total neuronal numbers (1), defective neural migration may explain this cell decrease as well as morphological differences in the brain.

Alpha Tubulin Conditional Knockout Mice

Unpublished observations of the *Tα1tubulin-Cre/Ikbkap* CKO mice used in this study reveal that compared to wild type mice, they are much smaller in size, have scoliosis, develop ataxic gait, and die earlier. Disruption of CNS motor areas is indicated by the presence of hind limb grasping behavior when suspended by the tail, unlike control mice, who splay their limbs. In addition to behavioral differences observed on tests of anxiety and escape behavior, other behaviors seen exclusively in *Tα1tubulin-Cre/Ikbkap* CKO mice included repetitive jumping at the wall of the holding cage, hind limb dragging, and docility. Some *Tα1tubulin-Cre/Ikbkap* CKO mice also display physical deformities including malformed jaws.

Further initial experimentation allowed for verification that the mouse models used for all analyses in the present study had *Tα1tubulin-Cre* active in the CNS, but not in the PNS, as indicated by crossing conditional knockout mice to $ROSA^{mT\text{-}mG/mT\text{-}mG}$ mice. When the *Ikbkap* floxed mice were crossed with *Wnt1-Cre* mice, all offspring died within 24 hours and were found to have markedly lower numbers of pain and temperature sensing neurons in the dorsal root ganglia (43). However, the *Tα1tubulin* mice displayed no differences in response to painful or high temperature stimuli, further indicating that the cells of these mice contained no deletion of *Ikbkap* in the PNS. Despite having *Ikbkap* ablated only from the CNS, the *Tα1tubulin-Cre/Ikbkap* CKO mouse model is a valuable tool for the evaluation of FD as they display many of the same symptoms seen in the FD human patients. Furthermore, the isolation of the CNS as the only affected branch of the

nervous system allows for study of *Ikbkap* deletion effects solely on this system without confounding influences from other branches.

Behavioral Observations in *Tα1tubulin-Cre/Ikbkap* Conditional Knockout Mice

Pilot behavioral studies were performed and suggest that behavioral differences exist between *Tα1tubulin-Cre/Ikbkap* CKO mice and controls, and that these differences may be explained by a decrease in anxiety levels or in comprehension of danger in the *Tα1tubulin-Cre/Ikbkap* CKO mice. The open field test, in which mice are placed in a four-walled, square box with an open top, revealed that while the control mice tended to hug the walls, affected mice actually spent more time in the center of the box than on the sides. Healthy mice hug the walls as a natural predation avoidance tactic (46). However, the affected mice do not seem to have this instinct, suggesting that either they experience less anxiety, or they simply do not comprehend the implications of being in the open like their control counterparts do, leaving them more vulnerable to natural selection.

The increased exploratory behavior in *Tα1tubulin-Cre/Ikbkap* CKO mice was also observed in preliminary tests using the elevated plus maze (55). This apparatus consists of a platform in the shape of a plus sign, where two arms are surrounded by walls, and thus are more sheltered from predation, and the other arms are simply straight, open, and elevated platforms with no protection. While the control mice quickly migrated to the protected arms where they tended to remain throughout the study, the affected mice spent more time in the open arms than the protected, performed more head dips below the platform, an exploratory behavior, and spent more time mobile than the controls did.

These findings indicate CNS alterations in the *Tα1tubulin-Cre/Ikbkap* CKO mice as manifested by reductions in anxiety or in diminished comprehension of the vulnerability of being in the open space as indicated by enhanced exploration.

Structures of Interest in *Tα1tubulin-Cre/Ikbkap* CKO Mice

Lateral Ventricles

The lateral ventricles are cavities in the brain containing cerebral spinal fluid (CSF) and are devoid of neural matter. They form from the most anterior part of the neural tube during development (51). The lateral ventricles communicate with the third, and indirectly with the fourth ventricles via a canal referred to as the intraventricular foramen of Monro. This ventricular system is responsible for both the production of cerebral spinal fluid via the choroid plexi, and its circulation through the brain (7). This circulation serves a multitude of crucial functions including removing toxins and metabolic waste from the CNS where it is absorbed back into the blood stream, protecting brain tissue from damage, and increasing the buoyancy of the brain inside the skull (52). Because preliminary observations revealed striking and obvious enlargement of the lateral ventricles of the mutant mice, this was the part of the ventricular system that was focused on in the present study. Though the lateral ventricles are crucial to healthy brain function, when they become abnormally enlarged, effects such as impaired cognition may result. In the case of hydrocephalus, where the ventricles may be enlarged because of an excess of cerebral spinal fluid due to improper drainage, excess production of CSF, or stenosis, frontal lobe function is especially impaired (13). Ventricular

enlargement also correlates strongly with Alzheimer's Disease and Mild Cognitive Impairment (14), where the enlargement of the ventricles is due to tissue atrophy rather than increased fluid levels and pressure in the brain. In both cases, cognition is somewhat impaired, possibly due to a compensation of other brain structures whose territory is overtaken by the ventricles. If there is significant enlargement of the lateral ventricles in the *Ta1tubulin-cre/Ikbkap* conditional knockout mice, determining whether the effect is due to developmental issues, progressive neurodegeneration, or hydrocephalus, will be instrumental in understanding the mechanism of disease progression in Familial Dysautonomia.

Corpus Callosum

The corpus callosum is a large bundle of fibers containing axons from the frontal, parietal, occipital, and temporal cortices. As the largest axonal pathway in the brain, the corpus callosum allows for communication between the left and right hemispheres and the homologous structures within each (53). Such interhemispheric communication is crucial for integrating sensory, motor, and visual inputs as well as for certain low and high-level cognitive functions (12). In order to determine whether the deficits seen in FD concerning these functions might be due to a corpus callosum insult, this structure was measured in the *Ta1tubulin-Cre/Ikbkap* CKO mice and compared to control mice.

Lateral Amygdaloid Nucleus

In efforts to elucidate the cause of observed behavioral differences in the mutant mice which suggest reduced levels of anxiety on tasks such as the open field test, and

elevated plus maze, investigation of the morphology of the lateral amygdaloid nucleus (LA) was performed. The lateral amygdaloid nucleus serves as the sensory gateway to the rest of the amygdala, delivering input and allowing other regions such as the central nucleus to produce physiological responses to a given stimulus (6). As such, it is hypothesized that if the LA structure is altered, certain stimuli that produce anxiety in healthy mice, such as open spaces, or being suspended by the tail, might not produce a physiological response in the affected mice and thus they would experience decreased levels of anxiety.

Thalamus

The Thalamus serves as the final processing center of ascending pathways before signals are sent to the neocortex, where the perceived sensations from the various sensory modalities are generated (10). Such modalities include all sensory systems with the exception of olfaction. Furthermore, the thalamus is crucial for motor function as it receives inputs from the cerebellum and basal ganglia. Once processed in the thalamus, information is then relayed to the motor cortex. The spinothalamic tract, a large ascending white matter tract, which runs from the spinal cord to the ventral posterior nucleus of the thalamus, carries information about pain and temperature, which is eventually relayed to the primary somatosensory cortex (16). When the spinothalamic tract or the thalamus itself is lesioned, these modalities may be impaired (10). Because individuals with Familial Dysautonomia have decreased pain and temperature sensation, motor deficits, and other possible sensory dysfunctions, examining the thalamus and its morphological relationship to the neocortex may provide insight into the communication

between these structures in the *Ta1tubulin-Cre/Ikbkap* CKO mice, and furthermore, into the etiology of the aforementioned symptoms. While the *Tα1tubulin-Cre/Ikbkap* CKO mice used in the present study have *Ikbkap* deleted only from the CNS, and preliminary studies have demonstrated that pain and temperature sensations remain intact, the thalamus, and its relationship with the neocortex, may still be affected as it is part of the CNS.

Hippocampus

The hippocampus is crucial for forming and consolidating memories, particularly long-term and spatial memories. Though there have not been noted memory alterations in FD patients, the *Ta1tubulin-Cre/Ikbkap* CKO mice tested on previous behavioral studies tended to explore their surroundings much more than controls do (55), which suggests increased use of spatial memory, but possible impairment of function as this increased exploratory behavior could be indicative of increased latency to learn the spatial environment. There is evidence that enhanced spatial memory results in enlargement of the hippocampal structure via experience-dependent usage in both animals and humans (2, 22). Furthermore, enlarged hippocampi have been observed in patients with autism (19), and there is evidence of comorbidity of this disorder and FD. Although there is currently no evidence of an enlarged hippocampus in FD humans, the hippocampus size was analyzed and compared to control mice in efforts to elucidate whether this phenomena transfers to the *Tα1tubulin-Cre/Ikbkap* CKO mice, and possibly to the human FD patients.

Barrel Cortex and Neocortex

The neocortex is made up of 6 distinct layers. In a given area of a normal brain, each of the layers has a consistent thickness relative to the others. The granular layers of the cortex (layers I-IV) are some of the last parts to develop in the brain. Cells must migrate the furthest from the ventricular zone to reach these layers, as the cerebral cortex develops in an inside-out pattern with neurons migrating along radial glia to reach their respective final destinations (20). If there is a defect in cortical layering in the *Tα1tubulin-Cre/Ikbkap* CKO mice, as measured by comparing the granular layers of the cortex to the supragranular layers, this will provide evidence suggesting that the observed morphological differences and deficiencies in the mutant mice are due, at least partly, to a migrational deficit.

Dorsal Motor Nucleus of the Vagus Nerve

The dorsal motor nucleus of the vagus nerve (DMNX; cranial nerve X), is a cluster of cholinergic cells that are responsible for sending parasympathetic projections to many of the body's major organs (Figure 1), regulating their functions (44). Because FD patients suffer from tachycardia and other heart arrhythmias, the DMNX was examined. A deficit in DMNX activity may explain the observed tachycardia as well as the digestive issues seen in patients, as the DMNX also projects to the pharynx and gastrointestinal tract.

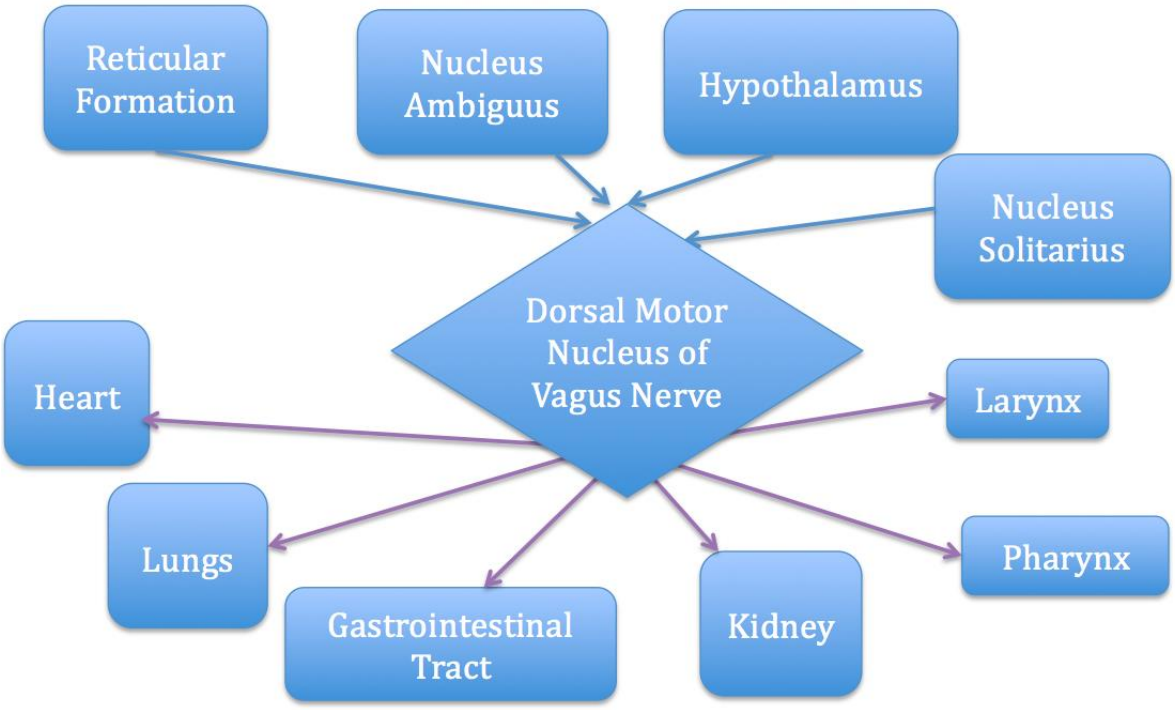

Figure 1. Afferent (above the diamond) and efferent (below the diamond) projections to the dorsal motor nucleus of the vagus nerve. This cholinergic nucleus sends parasympathetic preganglionic projections to postganglionic neurons in the organs seen in the figure. This innervation acts to slow the heart rate, promote digestion, and results in bronchial constriction (56).

Altered Brain Morphology in FD

Apoptosis Hypothesis

Preliminary studies suggest that *Tα1tubulin-Cre/Ikbkap* CKO mice have enlarged lateral ventricles. If the present study confirms this observation, it will be important to understand whether this effect is a result of hydrocephalus, increased cell death and tissue atrophy in the mutant mice, or whether this and other morphological differences are a result of deficient migration of neurons to their appropriate destinations during development. Another possibility is that the mutant mice may experience diminished

neurogenesis. There is evidence suggesting that reduced expression of IKAP results in activation of p53-pathways, promoting apoptosis in the PNS (4). If this diminished neurogenesis also occurs in the CNS, it would support an apoptotic mechanism in FD that could be responsible for the increased lateral ventricle size and any other atrophy seen in the central nervous system.

Cell Migration Hypothesis

Since Elongator has been implicated in cell motility and migration, it is possible that reduced levels of IKAP results in defective cortical layering and improper formation of other structures during development, leaving more ventricular space where gray matter should be. Indeed, it has been shown that reduced levels of IKAP results in histone H3 hypoacetylation, reducing transcriptional elongation of a number of target genes that are crucial for cell motility (11). Furthermore, cell migration assays using cells from FD patients indicated defective migration (11). A migrational defect could be the cause of many of the neurodevelopmental defects seen in patients and potentially in the *Tα1tubulin-Cre/Ikbkap* CKO mice. For this reason, cortical layering patterns were analyzed in efforts to determine whether a defect might exist.

Neurogenesis Theory

A third possible explanation for an observed decrease in brain matter in the mutant mice is that the reduction of IKAP results in impaired neurogenesis. In *Wnt1-Cre Ikbkap* knockout mice, where *Ikbkap* was knocked out of the PNS as well as regions of the CNS, neurogenesis was drastically reduced in the dorsal root ganglia, where numbers

of trkA^{+} (neurotrophic tyrosine kinase receptor type 1) nociceptors and thermoreceptors were roughly half that of the control mice. These results indicate a crucial role for IKAP in neurogenesis (43). Furthermore, there is evidence that IKAP is required for neurogenesis in the peripheral nervous system, whereby neural crest cells that over-express the c-terminus of the IKAP mRNA both migrate less efficiently and fail to differentiate into neurons as frequently as control cells did (17). Should this hold true for neurogenesis in the CNS, it would offer an explanation for the difference in morphology between mutant and control brains; why some structures are affected while others develop normally would need to be elucidated.

Hydrocephalus Theory

While enlargement of the lateral ventricles in the *Ta1tubulin-Cre/Ikbkap* CKO mice could be due to hydrocephalus, there is little evidence that this occurs in the human FD patients. If other morphological differences are observed in the CNS, alternative hypotheses would need to be evaluated, since hydrocephalus is only able to account for the structural changes seen in the ventricles.

CHAPTER 2

MATERIALS AND METHODS

Genetic Knockout Strategy

All procedures were approved by the Montana State University Institutional Animal Care and Use Committee. Mice were obtained from the International Knockout Mouse Consortium. Since mice that were homozygous for a *frt*-flanked *LacZ Ikbkap* reporter which prevents IKAP expression before the 4th exon of *Ikbkap*, died by embryonic day 10, flippase-mediated recombination was used to remove the β-galactosidase cassette, which rescued *Ikbkap* expression (Figure 2). A conditional knockout model was created using the new allele, which contains *LoxP* sites flanking the *Ikbkap* coding sequence, which was then removed using *Cre* recombinase. The homozygous *Ikbkap* conditional knockout mice were then crossed to hemizygous *Tα1tubulin-Cre* mice to produce a mouse model that is homozygous for the *Ikbkap* knockout only in tissues where Cre is expressed.

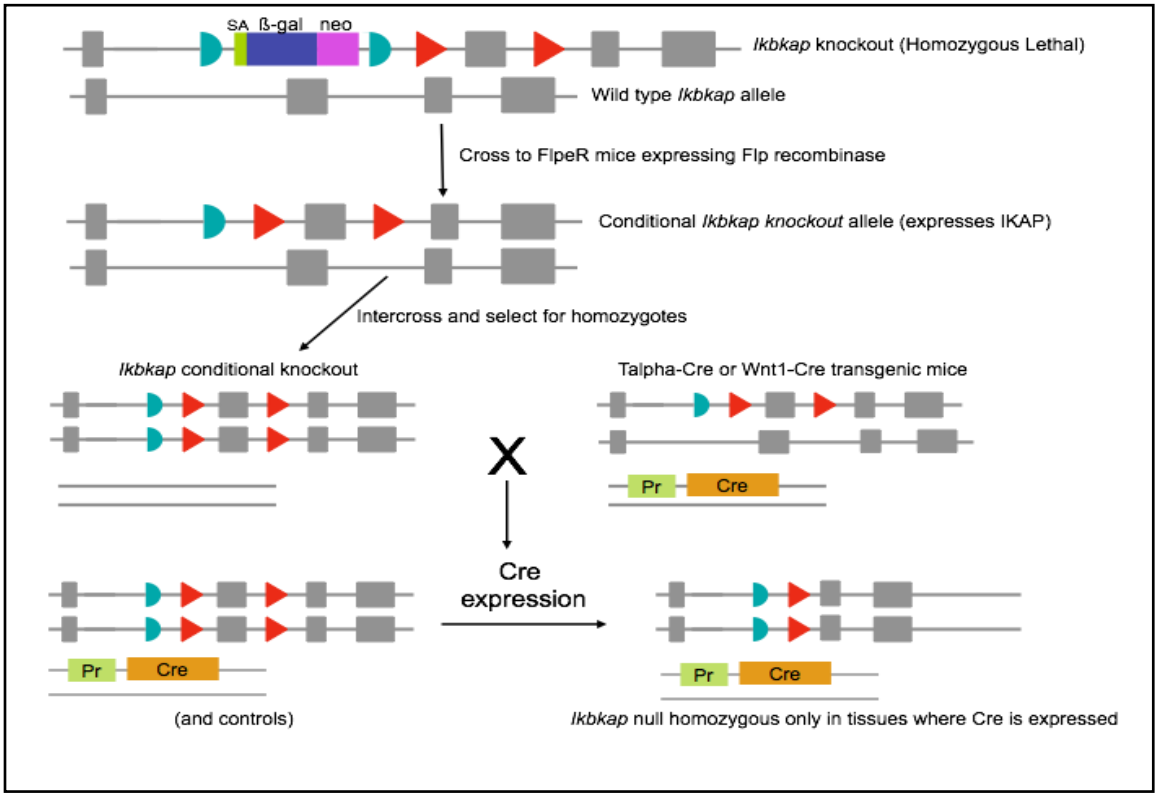

Figure 2. Genetic Knockout Strategy employed to create α-Tubulin conditional knockout mouse models of Familial Dysautonomia.

Tissue Preparation

Mice were sacrificed and tissues fixed by means of transcardial perfusion. Animals were placed into a bell jar containing approximately 1-2 ml of isofluorane as a general anesthetic. Approximately 35 ml of 1X Phosphate Buffer Solution (PBS) was pumped through the animal's vasculature, followed by 35 ml of ice cold 4% paraformaldehyde solution. The organs were dissected out and placed into vials containing 4% paraformaldehyde and fixed for 24 hours at 4°C. Following fixation, tissue was stored in 30% sucrose in .1M phosphate buffer solution until sectioning. Mice that were not perfused had the brain dissected out and fixed as above.

Tissue Sectioning

Brains were sectioned one of two ways. In the first method, brains were imbedded in Optimal Cutting Temperature (OCT) gel blocks and flash frozen. Next, they were cut coronally at 20 µm per section on a Cryostat and sections placed onto slides which were stored at -20°C. Because this method somewhat compromised the integrity of the tissue, some brains were cut using a sliding microtome instead. Coronal sections of 40 µm were then collected and placed into 9 by 10 well trays filled with cryoprotectant solution and stored at 20°C until used. The cryoprotectant solution was made up of 10g polyvinylpyrrolidone, 300 ml ethylene glycol, 300g sucrose, and 500ml dH_2O containing 1.59g monobasic sodium phosphate and 5.47g dibasic sodium phosphate.

Tissue Mounting

Once free floating sections had been stained using immunohistochemistry (see protocol on pg. 17), they were placed onto Superfrost plus slides using a fine tipped paintbrush and a dissecting microscope to straighten out the sections and remove dust particles and other debris. Slides were then stored in slide folders and allowed to air dry before being coverslipped.

Cresyl Violet Staining Protocol

In order to visualize neural structures within the brain, sections were stained with Cresyl violet, which stains all Nissl bodies within cells. Cresyl violet solution was made up using 1.25g cresyl violet acetate, 0.75ml glacial acetic acid, and 250ml warm dH_2O.

The solution was then cooled and filtered before use. Slides were double stained in order to optimize contrast.

Immunofluorescence Protocol:

All *Tα1tubulin-Cre/Ikbkap* CKO mice were paired with age-matched littermate control animals whose tissue was processed at the same time using the same protocols. Slides and free floating sections were fluorescently stained using the following protocol for amplification:

1) Slides were fixed in 4% Paraformaldehyde for 2 minutes*
2) 10 minute soak in PBS to remove any remaining cryoprotectant solution or OCT.
3) 2x2 minute washes in PBS
4) Block for 20 minutes in Animal Free Blocker (Vector)
5) 3x6 minute washes in PBS
6) Incubate in primary antibody diluted in Animal Free Blocker overnight at room temperature on shaker
7) 6x7 minute washes in PBS
8) Incubate in biotinylated secondary antibody for 1 hour at room temperature on shaker
9) 6x7 minute washes in PBS
10) Incubate in streptavidin fluorescent antibody for 1 hour at room temperature on shaker
11) Wash 3x10 minutes
12) Mount on slides if free floating
13) Coverslip with Prolong Gold (Invitrogen)

*This step was omitted for free-floating sections.

Primary antibodies used included polyclonal goat α-Cholineacetyltransferase (Millipore) at 1:200, monoclonal mouse α-Neuronal Nuclei (NeuN;Millipore) at 1:500, polyclonal rabbit α-Neuropeptide Y (Calbiochem) at 1:1000, and polyclonal rabbit α-Cleaved Caspase 3 (Cell Signaling Technology) at 1:250.

Biotinylated secondary antibodies were all purchased from Vector and were used at 1:300. These included goat α-rabbit IgG, goat α-mouse IgG, and rabbit α-goat IgG. The streptavidin Alexa Fluor ® 488 antibody was purchased from Life Technologies and was used at 1:500. Other fluorescent secondary antibodies used included Alexa Fluor ® 488 donkey α-goat IgG (Life Technologies) used at 1:2000, Alexa Fluor ® 568 goat α-mouse IgG (Invitrogen) used at 1:2000, and Alexa Fluor ® 568 goat α-rabbit IgG (Invitrogen) used at 1:2000, and DAPI used at 1:3000.

All antibodies were diluted in Animal Free Blocker (Vector), used at 1:4 in dH_2O.

Confocal Microscopy

Sections were analyzed and photographed using a Leica confocal microscope with the 488 and 568 laser intensities on identical settings for both control and mutant sections of the same stains. Z-stack images were obtained using Leica Application Suite Advanced Fluorescence software, and staining intensities were measured using Image J. For ChAT staining, positive cells in the dorsal motor nucleus of the vagus nerve were quantified by hand and the two sections from each animal with the greatest number of cells were averaged to get one final number for each animal.

Photographing Nissl Stained Brain Sections

Sections were photographed using a camera on a Zeiss dissecting microscope attached to a computer with a 6X lens and additional adjustable magnification settings. AxioVision software was used to collect and organize photographs of the sections.

Settings on the microscope in the imaging program were adjusted to ensure collected images showed optimum clarity and contrast between white and gray matter to increase ease of identifying structures and nuclei.

Quantification of Staining Intensities

Neuronal Nuclei and Neuropeptide Y staining were quantified using Image J software. A histogram calculating amount of color (either red or green) compared to black in each image was created, and color values were recorded and analyzed.

Analysis of Structural Areas

Images were loaded into OsiriX version 5.6 image processing software for iOS. Regions of Interest (ROIs) for each brain section were physically outlined and the area of each calculated by the program in arbitrary units. An area measure for the corresponding hemisphere to each ROI was calculated as well. Numbers were recorded and ratios calculated in a Microsoft Excel spreadsheet. The Allan Mouse Brain Atlas (5) was used as a reference to ensure proper boundaries of sections were being outlined at various stereotaxic coordinates. For each structural measure, three serial sections were chosen 40 μm apart at identical coronal levels for each animal.

Lateral Ventricles

The boundaries for the lateral ventricles were drawn around the area where no brain matter was present, with the exception of choroid plexus. The regions used to

evaluate the lateral ventricles were sections chosen were where the fimbria was just medial to the lateral ventricle.

Corpus Callosum

The boundaries for the corpus callosum were drawn beginning in the center of the coronal section, just dorsal to the dorsal fornix and directly ventral to the cingulate bundle. The fiber bundles were then traced between the cortex and caudate putamen and tracing was stopped at the level of the rhinal fissure, directly above the claustrum.

Lateral Amygdaloid Nucleus

The lateral amygdaloid nucleus was traced beginning where the external capsule and amygdalar capsule split. The ventral end of the tracing was where the basolateral amygdalar nuclei began and a small fiber bundle separated the lateral from basolateral nuclei.

Thalamus

The thalamus was evaluated beginning at the most medial edge of the periventricular nucleus, then followed the medial edge of the medial habenula, and continued directly ventral to the hippocampal formation, medial to the fimbria and cerebral peduncle, and directly dorsal to the hypothalamus.

Neocortex Area

Cortical layers I through VI were measured beginning on the medial edge of the ventral part of the retrosplenial area of layer 1, down to the level of the rhinal fissure, and up the medial edge of layer 6.

Barrel Cortex and Neocortex Depths

The depths of the granular cortical layers were identified by the presence of large barrel cells in the barrel field of the primary somatosensory cortex. A straight line was drawn from the lateral edge of layer I to the bottom of the barrel field (layer IV), and compared to a second line drawn from the same point on the lateral edge of layer I that extended to the bottom of layer VI.

Hippocampus

The boundaries for analysis of the hippocampus were the area dorsal to the third ventricle, and immediately ventral to the dorsal fornix and corpus callosum. The structure was traced following the lateral edges of the stratum oriens of CA fields 1, 2, and 3 and continued along the ventral edge of the dentate gyrus.

Data Analysis

Ten control and 11 mutant mice were used for each region of interest (ROI). Each structural measure was divided by a measurement of the corresponding hemisphere to generate a percent area measure. This controlled for overall size differences between each brain. Each ROI and hemisphere area was measured in three separate sections

approximately 40 µm apart, chosen based on the size and morphology of each structure, consistent between animals. The ROI areas were then divided by the hemisphere areas, and the averages of these three final area measures were calculated for each animal to yield a single, final value. To quantify staining intensity for immunohistochemistry, images were analyzed using Image J software, where a value was calculated based on the amount of color versus black present in each image.

Each of the control values for a given ROI was compared to the corresponding values for mutant animals using an unpaired two-tail t-test, with an alpha level less than 0.05 considered significant. Measures of standard deviation and standard error were also recorded.

CHAPTER 3

RESULTS

Overall Hemisphere Size

There was no significant difference found when the areas of the hemispheres were measured using coronal sections (Table 1; t(20)=1.57, p=0.130).

Lateral Ventricle Areas

The mean lateral ventricle size for the control mice was 1.9% of the total hemisphere area (Table 1). In contrast, the mean lateral ventricle size for the mutant mice was significantly greater, where 7.6% of their hemisphere areas were composed of the lateral ventricle. This difference was significant (Table 2; t(20)=-3.20, p=0.004).

	Wild Type Mice ± SD (n=10)	*Ta1tubulin-Cre/Ikbkap* CKO Mice ± SD (n=11)	p
Animal Weight (g)	29.6 ± 5.0	16.2 ± 4.9	<0.001*
Size of Hemisphere (mm^2)	44.7 ± 17.9	32.3 ± 17.11	0.13
Percent Lateral Ventricle	1.90 ± 0.017	7.61 ± 0.054	<0.005*
Percent Corpus Callosum	3.62 ± 0.009	2.51 ± 0.006	<0.001*
Percent Lateral Amygdaloid Nucleus	2.54 ± 0.007	1.63 ± 0.005	<0.008*
Percent Thalamus	19.21 ± 0.03	16.82 ± 0.02	0.08
Thalamus:Neocortex Ratio	0.665 ± 0.17	0.651 ± 0.43	0.84
Granular Cortex:Supragranular Cortex Ratio	0.481 ± 0.03	0.466 ± 0.03	0.30
Percent Hippocampus	10.93 ± 0.017	15.0 ± 0.025	<0.005*

Table 1. Average size of brain structures in control and mutant mice. Unless otherwise specified, all measures are of the area of the structure over the area of the hemisphere. Ratios reflect within-animal calculations. p-values followed by an asterisk are statistically significant with an alpha level of 0.05.

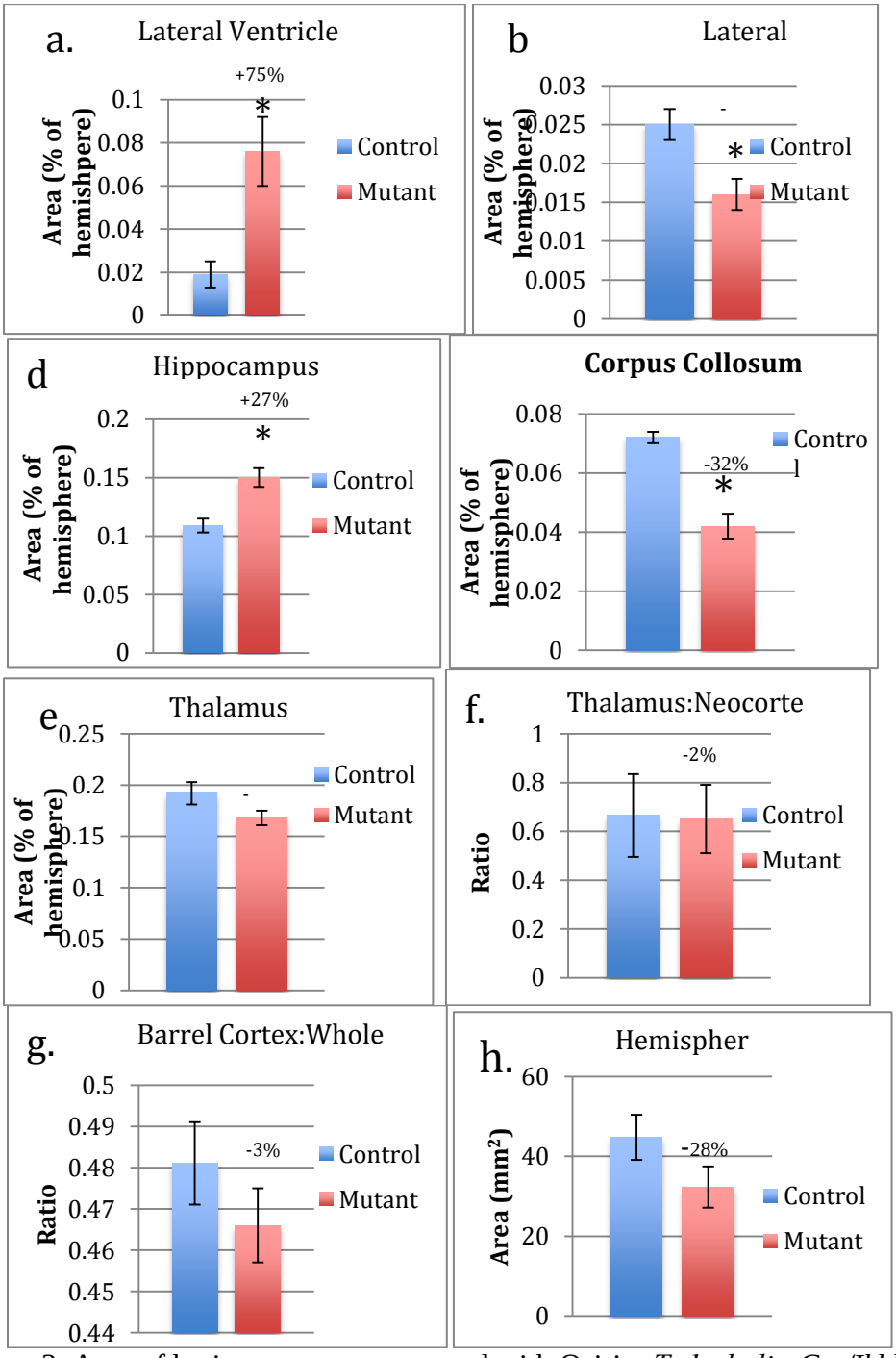

Figure 3. Area of brain structures measured with Osirix. *Tα1tubulin-Cre/Ikbkap* CKO mice (red) have significantly smaller corpus callosum (b) and lateral amygdaloid nucleus (c), while they show significantly increased size of the lateral ventricles (a) and hippocampus (d). Differences in thalamus size (e), ratios of thalamus to neocortex (f) and of barrel cortex depth to whole cortex depth (g) as well as overall hemisphere sizes (h) did not reach significance. The graphs indicate mean measures ± SEM. *p<0.05.

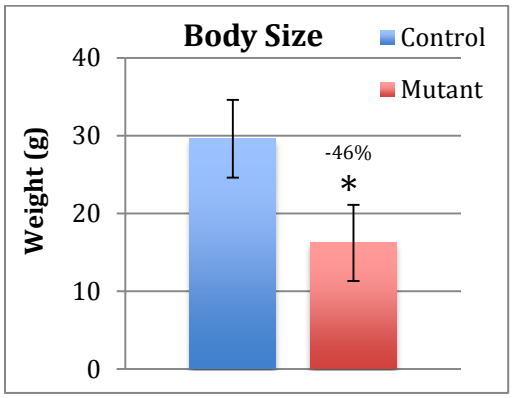

Figure 4. Average weight of control and *Ta1tubulin-Cre/Ikbkap* CKO mice. On average, adult mutant mice (red) weighed 46 percent less than their control counterparts (t(20)= -11.90, p = 0.0001).

a.

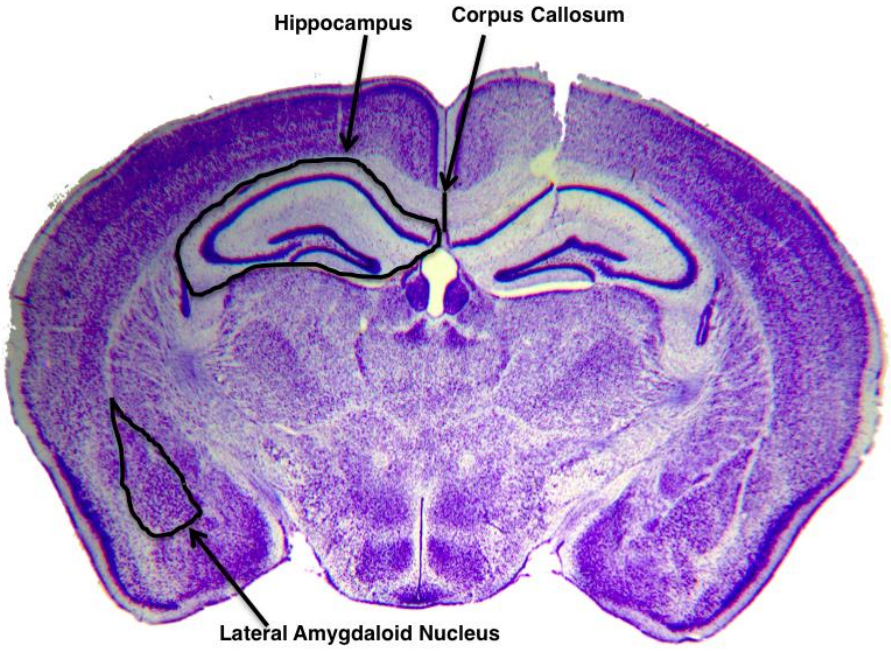

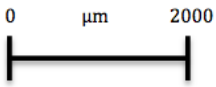

Figure 5 Continued

b.

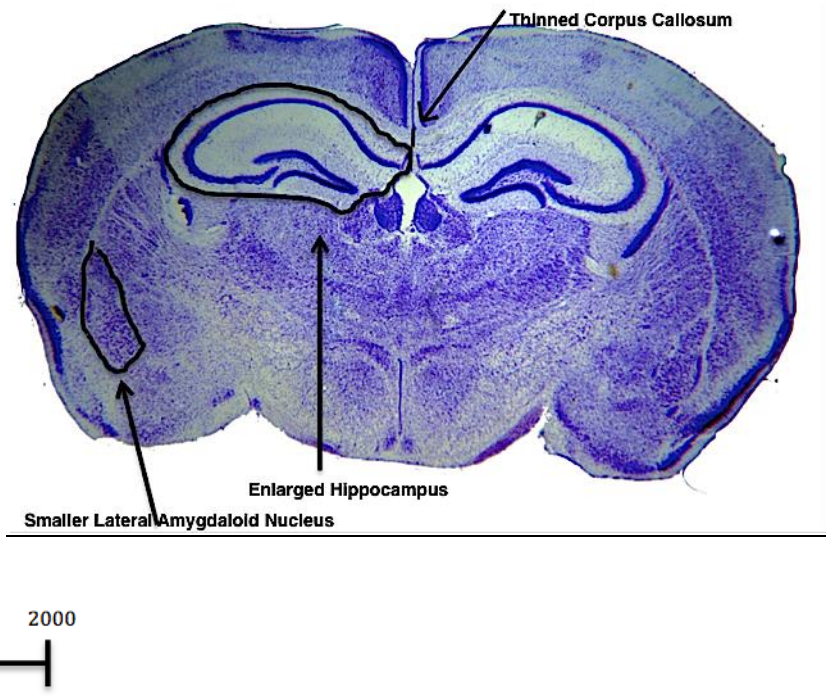

Figure 5. Coronal Nissl stained section of a control mouse brain (a) and a mutant brain (b). The Corpus Callosum, Lateral Amygdala, and hippocampus are outlined, and differences indicated in the second image. The relative sizes of the brain are true to scale, and images were taken at identical magnification.

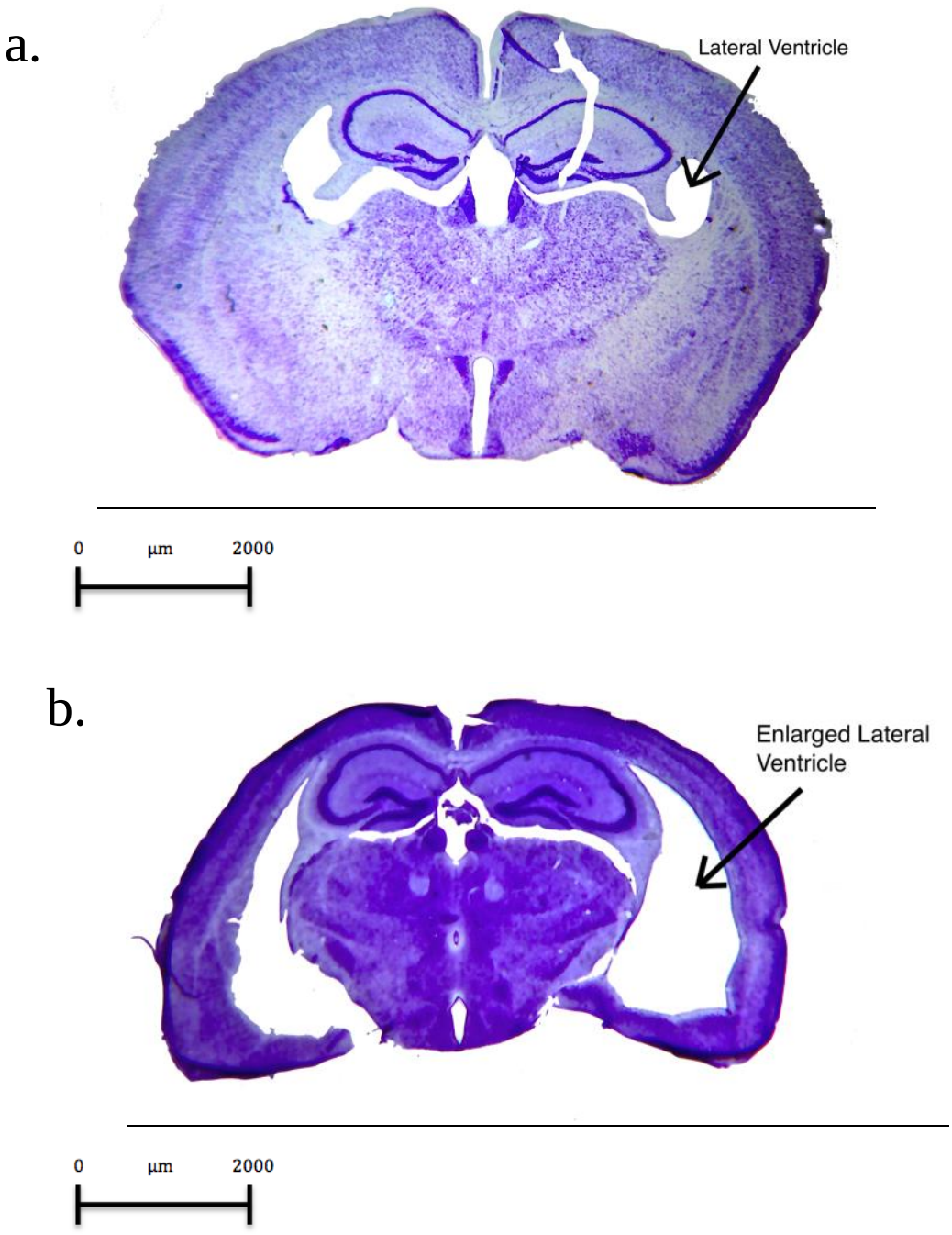

Figure 6. Comparison of lateral ventricle size in control (a) and mutant (b) mice. The lateral ventricle takes up an average of 7.6% of the total hemisphere area in mutant mice, and an average of 2% in controls. Relative sizes of the brains are true to scale, and images were taken at identical magnification.

Corpus Callosum Areas

The overall area of the corpus callosum was decreased in the mutant mice compared to their control counterparts (Figure 3). The average corpus callosum size for the control mice was 3.6% of the hemisphere area, whereas for the mutant mice it was only 2.5%. This difference was significant ($t(20)=3.23$, $p=.005$).

Lateral Amygdaloid Nucleus Areas

The average value for the Lateral Amygdaloid Nucleus was significantly smaller in the mutant mice compared to controls ($t(20)=2.98$, $p=0.008$) The mean value for wild type mice was 2.5% of the hemisphere area. In the *Ta1tubulin-Cre/Ikbkap* CKO mice, this value was 1.6% of the total hemisphere area (Figure 3).

Thalamus Areas

The average size of the thalamus as a proportion of the hemisphere was not significantly different between mutant and control mice ($t(20)=1.83$, $p=.08$), nor was average size of thalamus relative to the neocortex area (Figure 3). Control mice had a mean value 19% of the hemisphere area composed of thalamus compared to 17% thalamus for mutant mice.

Ratio of Cortical Layers I-IV to Infragranular Layers

There were no significant differences between the control and mutant mice ($t(20)=0.19$, $p=0.83$) regarding the ratio of supragranular and granular (layers I-IV) cortex to infragranular cortex (layers V and VI).

ChAT positive cells in the Dorsal Motor Nucleus of X

There were significantly greater numbers of ChAT positive cells in the DMN of X in control mice than there were in affected mice (Figure 8; $t(13)=8.12$, $p=0.0001$). Additionally, the signal of ChAT positive cells was also somewhat brighter despite the images being taken with identical laser intensities and magnification (Figure 7).

a.

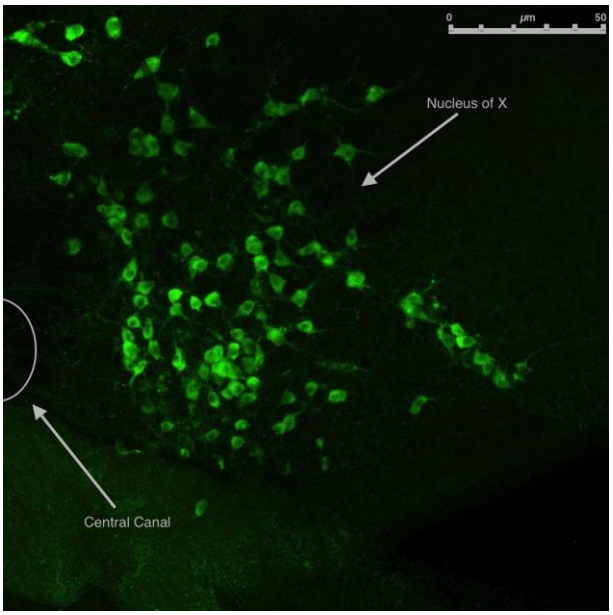

Figure 7 Continued

b.

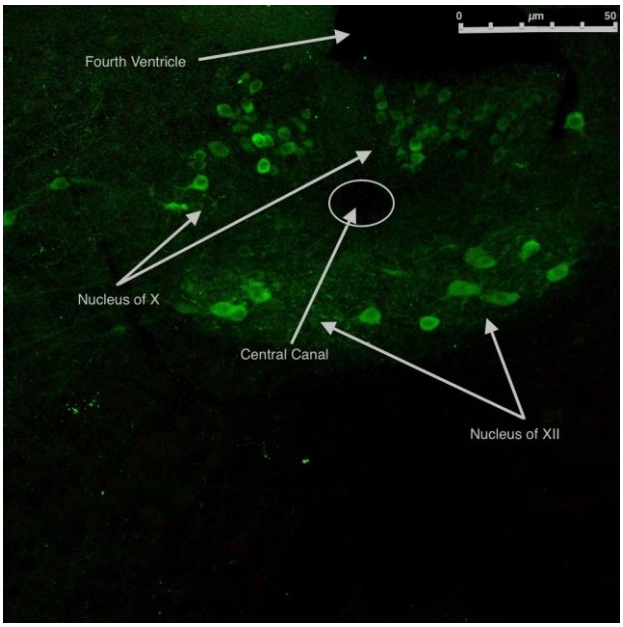

Figure 7. Cholineacetyltransferase (ChAT) staining in control (a) and mutant (b) brains at the level of the dorsal motor nucleus of the vagus nerve (nucleus of X). Both images were taken at 20X magnification, but due to size differences between the two animals, the control image shows only the right hand nucleus of X with the fourth ventricle in the upper right hand corner, while the mutant image has both the left and right nucleus of X on either side of the central canal, as well as the nuclei of XII below, which contain the larger, more sparse ChAT positive cells. Note scale bars in upper right hand corners, which are magnified 4X and represent 50 microns for comparison purposes.

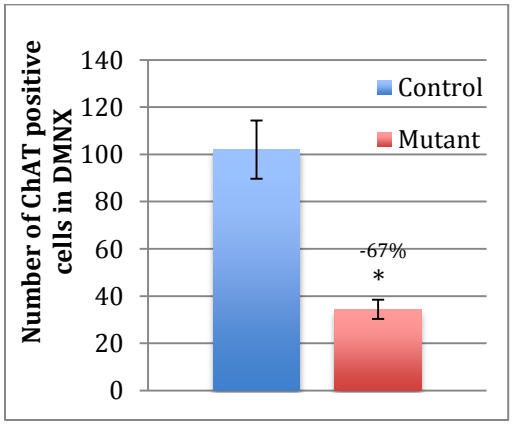

Figure 8. Number of ChAT positive neurons in the dorsal motor nucleus of the vagus nerve of control (n=6, blue) compared to the mutant mice (n=7, red). * $p<0.001$.

Neuronal Nuclei Staining

As depicted in Figure 9, the Neuronal Nuclei (NeuN) staining intensity in control somatosensory cortex appears slightly brighter than in mutant cells. However, in the CA1 field of the hippocampus, this trend is reversed, with mutant cells expressing NeuN more brightly. This observation when quantified for brightness using ImageJ software, did not achieve significance.

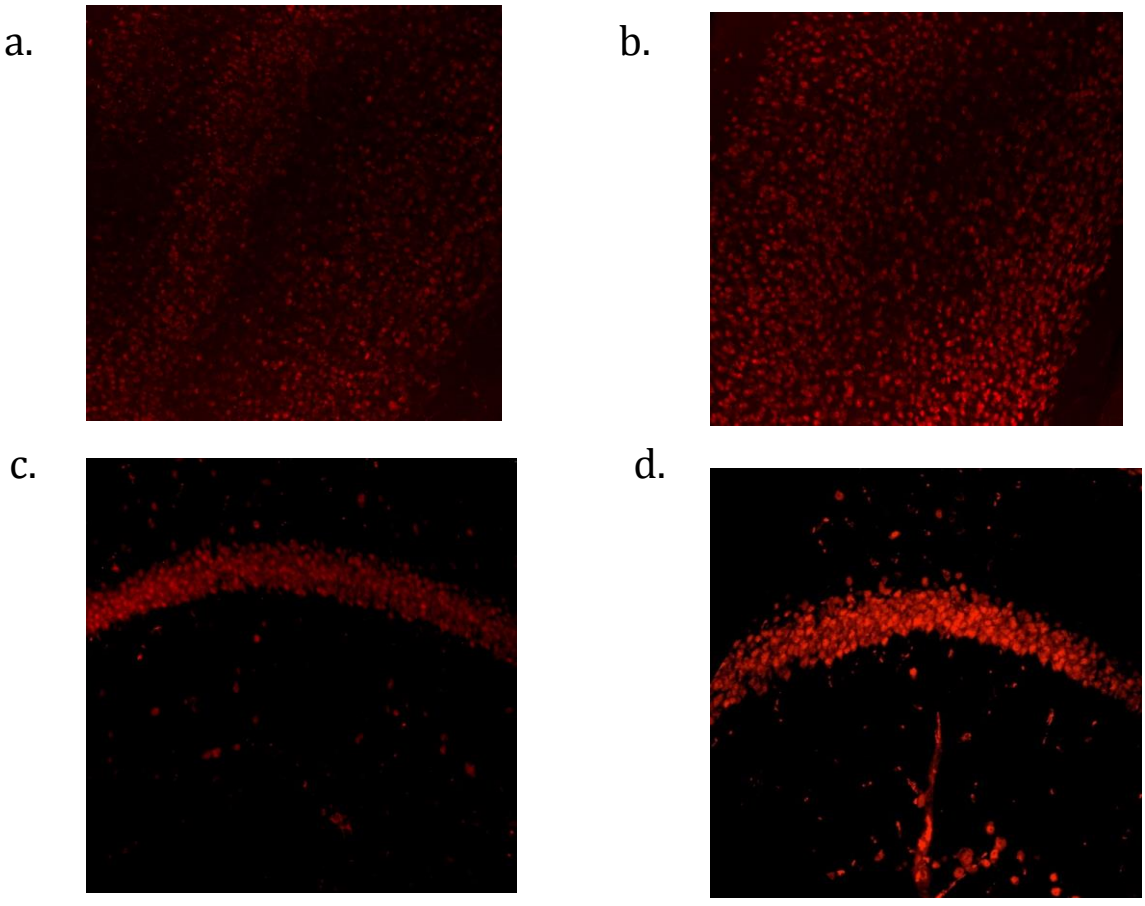

Figure 9. Neuronal Nuclei staining in control somatosensory cortex (a) and *Tα1tubulin-Cre/Ikbkap* CKO somatosensory cortex (b) and in the CA1 field of the hippocampus in control (c) and mutant (d) brains.

Neuropeptide Y Staining

Immunohistochemical staining of Neuropeptide Y (NPY) revealed more intense staining in the mutant hypothalamus, particularly in the zona incerta (Figure 10) and paraventricular nucleus. While this trend was consistent across animal pairs tested, the small number of subjects analyzed (three controls and three mutants) precluded statistical evaluation of these data.

a.

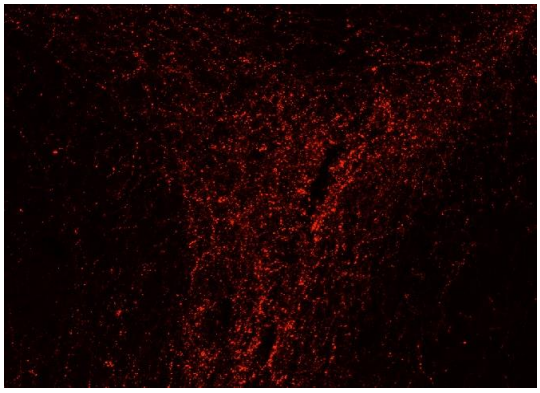

b.

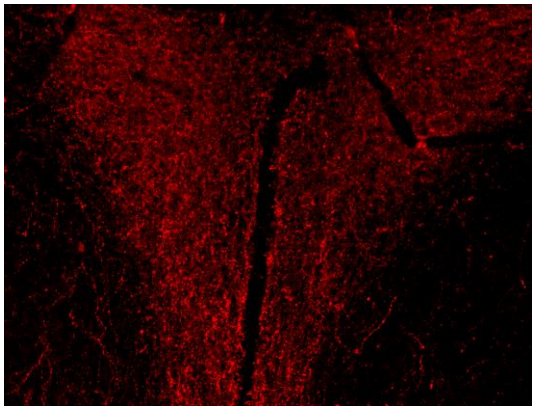

Figure 10. Neuropeptide Y stain in the hypothalamus of control (a) and mutant (b) mice in the region of the paraventricular nucleus.

CHAPTER FOUR

CONCLUSIONS

The results of the morphological analyses and immunohistochemical staining reveal significant differences between the control and *Ta1tubulin-Cre/Ikbkap* CKO central nervous systems, which may be responsible for some of the behavioral alterations and health deficiencies seen in the affected mice. It was an unexpected result that the hemisphere sizes were not different, particularly given the significant difference in body weights between the mutant and control mice. This could be due to an inadequate method for analyzing the hemisphere size. Since it was consistently observed that control hemispheres appeared much longer than mutants before the brains were sectioned, this measure should be re-evaluated. Perhaps measuring the length of the hemispheres would allow the size differences to be captured in the results. Furthermore, volumetric measures should be done, subtracting the volume of the ventricles to get a true measure of brain volume that can be compared between controls and mutants. Despite the possible methodological shortcoming present in hemisphere analysis in this study, research has shown that within species, overall brain volume is relatively conserved regardless of body size of the individual (40). Perhaps the comparable brain size makes the structural differences observed even more convincing, as they cannot be attributed to overall brain volume differences, but rather are unique to each particular structure and are conserved between mutant mice. These findings are important because they indicate that deletion of *Ikbkap* in the CNS alone is sufficient to reproduce many of the classic symptoms seen in

patients with FD, even though the PNS has traditionally been the research focus in the disease.

The cortical layering as analyzed by comparison of barrel cortex depth to whole cortex depth was the same for *Tα1tubulin-Cre Ikbkap* CKO mice and controls, providing evidence that the observed morphological deficiencies in the affected mice are not due to deficient cell motility and migration. Since the cerebral cortex is among the last regions of the brain to develop, the fact that it is properly layered in the *Tα1tubulin-Cre Ikbkap* CKO mice indicates normal cell migration, even to the outermost layers. Taken together, these data support a role for apoptosis and neurogenesis as mechanisms for enlargement of the lateral ventricles observed in the *Tα1tubulin-Cre Ikbkap* CKO mice .

Despite the lack of evidence for migrational deficits in the *Tα1tubulin-Cre*/*Ikbkap* CKO CNS, preliminary observations did identify the presence of focal ectopias in the mutant somatosensory cortex. Focal ectopias, specifically molecular layer ectopias, occur when cells migrate beyond the appropriate cortical layers into layer I, which is normally devoid of cell bodies (32). This disorder has been associated with cognitive deficits such as psychomotor retardation and dyslexia in humans. In mice that have induced focal ectopias, improved reference memory, but impaired working memory was observed as were seizures (33). The ectopias in the *Tα1tubulin-Cre*/*Ikbkap* CKO mice were not quantified, but this observation should be pursued in future studies since the presence of such ectopias would indicate altered neuronal migration, and could also provide further insight into cognitive differences between control and mutant mice.

Significantly lower numbers of ChAT positive cells in the DMNX indicate a decrease of parasympathetic innervation of the various organs to which this nucleus projects. This could provide an explanation for the observed tachycardia in FD patients, since normal heart rate is maintained by a balance between sympathetic and parasympathetic innervations (31) and for the disruption in digestive processes seen in FD patients. Future research should focus on the DMNX as a therapeutic target for treating symptoms in FD associated with the organs it innervates.

The most significant difference in morphology between the mutant and control brains was that of the lateral ventricle size. The increase in size of lateral ventricles in affected brains compared to controls is likely explained by neuronal degeneration, since decreased IKAP levels have been associated with apoptosis in the nervous system, and by decreased neurogenesis in development. This increased space in the brain certainly compromises the space, and thus the functions, of other surrounding structures. Investigation of the lateral ventricle size in embryonic brains falls beyond the scope of the present study, but this should be investigated in efforts to understand at what developmental stage degeneration becomes substantial, or whether this altered feature of CNS morphology develops along with the brain in utero. Furthermore, investigation of hydrocephalus as a potential cause for the enlargement of the ventricles should be done, in efforts to further elucidate the disease mechanism behind this finding. While hydrocephalus is often the cause of enlarged ventricles, this mechanism alone fails to account for other morphological differences in the CNS that are observed in the *Ta1tubulin-Cre/Ikbkap* CKO mice such as the enlarged hippocampus, smaller lateral

amygdala, and thinner corpus callosum. In order to conclusively rule out hydrocephalus as a cause, computed tomography (CT) scans should be performed and pressure sensors implanted in live *Ta1tubulin-Cre/Ikbkap* CKO mice in efforts to analyze CSF volumes and resulting intracranial pressures to determine whether hydrocephalus is in fact a cause of the enlargement of the lateral ventricles.

The lateral amygdaloid nucleus was found to be smaller in the *Tα1tubulin-Cre Ikbkap* CKO mice compared to controls, but the impact this has on symptomology and behavior remain to be elucidated. Perhaps the diminution of the LA contributes to the reduction in anxiety and increased docility observed in other studies that have evaluated the *Tα1tubulin-Cre*/*Ikbkap* CKO mice (55). The amygdala has been shown to be atrophied in Alzheimer's disease (37), and the neuronal size and overall volume are decreased in patients with bipolar disorder (38, 39). Symptoms of these effects include irregular motor behavior, anxiety and irritability. However, based on preliminary observations, the *Tα1tubulin-Cre*/*Ikbkap* CKO mice tend to be less anxious and more docile than their control counterparts. The studies described above found increased activation of the amygdala despite is smaller size, indicating that the structure perhaps compensates for the lack of volume via up-regulation of function, producing negative affect in the individual. It is possible that the *Tα1tubulin-Cre*/*Ikbkap* CKO mice instead under-utilize their amygdalae, producing the observed calm behaviors. Furthermore, two of the previous studies looked at the whole amygdala, while the present study focused only on the LA, which is the relay station to the rest of the structure. In order to elucidate

the role of the LA in FD symptomology, future research will need to analyze its activation *in vivo* compared to that of control mice.

Tα1tubulin-Cre/*Ikbkap* CKO mice have an enlarged hippocampal formation compared to controls, and were observed to be much more motile and displayed more exploratory behaviors on pilot studies using the open field test and elevated plus maze. Some studies have suggested that increased exploratory behavior could correlate with an enlarged hippocampus (18), though causality is difficult to determine. Additionally, compared to mice bred for high levels of aggression, non-aggressive mice tended to explore their surroundings in the open field test more, spent significantly more time motile overall, had more mossy fibers in their hippocampus, and larger volumes of field CA4 (18). These findings point to a connection between the hippocampus, aggression, and exploratory behavior, which should be investigated in future studies.

There is also evidence to suggest that the hippocampus is enlarged in individuals with autism (19), a finding that has been demonstrated in children, adolescents, and young adults. Creation of a mouse model of autism was accomplished by knocking out the *SCN1A* (sodium channel, voltage gated, type 1, alpha subunit) gene, which is responsible for encoding the alpha subunit of voltage-sensitive sodium channels (30). Interestingly, this gene is decreased four-fold in the *Ikbkap* conditional knockout mouse brains, suggesting a possible link between autism and FD. One explanation for the enlarged hippocampal formation in autistic individuals is use-dependent experience. Literature suggests that animals (21), as well as humans (22), with better spatial memory tend to have an enlarged hippocampus. Since studies have shown that the *Tα1tubulin-Cre*

Ikbkap conditional knockout mice spend more time motile and explore their surroundings more, it is possible that they develop better spatial maps, rely more on their spatial memory, and thus have an enlarged hippocampus compared to controls. Furthermore, it was demonstrated that compared to age matched controls, individuals with autism are superior at learning and reproducing a route map, both in terms of accuracy and speed with which they perform the task (23). If the mechanism of hippocampal enlargement in autism is common to that seen in the *Tα1tubulin-Cre*/*Ikbkap* CKO mice, the comorbidity of autism and FD could help explain this morphological finding.

While studies have failed to support to a developmental mechanism for the enlarged hippocampus in autism, mice that have a deficiency in the Kv1.1 protein (Potassium voltage gated channel subfamily A member 1), also present with a grossly enlarged hippocampus (24). Kv1 is encoded by the *KNCA1* gene, a member of the KCN gene family, a class of genes that synthesize potassium channels (25). Potassium channels are crucial for regulating the transmission of electrical signals, as well as cell proliferation. In their absence, cells may proliferate abnormally and become overexcited. In the hindbrain region, the *Tα1tubulin-Cre*/*Ikbkap* CKO mice used in the present study were found to have a 4.6 fold decrease in *KCNAB3* (voltage potassium channel subunit beta-3), also a member of the KCN gene family (47). This provides another possible mechanism for the enlargement of the hippocampus, and also indicates possible cell signaling deficits as a result. This reduction in *KCNAB3* may also result in over-excitation of neurons, which may provide a mechanism for the observed seizures in FD patients.

Mice that are homozygous for truncated Kv1 proteins present with motor disturbances that are progressive and they also have complex partial seizures after postnatal week 4. Along with the ventral cortex, the hippocampus becomes progressively enlarged and displays deficiencies in expression of brain derived neurotrophic factor (BDNF) and neuropeptides. Increases in number and size of neurons and astrocytes in the hippocampus, possibly as a result of the removal of the Kv1 brake-like regulation, may be the mechanism behind the enlargement of the structure (24).

Human FD patients experience cognitive deficits such as learning delays (45). The decrease in corpus callosum size in *Tα1tubulin-Cre*/*Ikbkap* CKO mice if conserved in FD human populations, may provide an explanation of some of the cognitive deficits including such learning disorders, as decreased corpus callosum volume may result in decreased communication between the hemispheres, and thus global deficits in cognition (41).

The decrease in corpus callosum size could also be provide insight into the mechanisms underlying the disorder agenesis of the corpus callosum (AgCC). In this condition patients either do not form, or form a much thinner and shorter, corpus callosum (15, 8, 9). Though the etiology of AgCC remains unclear, there is evidence that it could be the result of genetic factors such as trisomy 8, 13, and 18, as well as environmental factors such as maternal substance abuse or illness during pregnancy (15). Hereditary motor and sensory neuropathy associated with AgCC (HMSN/AgCC) results from a mutation in the gene *SLC12A6* (solute carrier family 12, member 6) which is a potassium-chloride co-transporter (8). This gene was not down-regulated in *Tα1tubulin-*

Cre/*Ikbkap* CKO mice, but other members of the solute carrier family such as *SLC5A7*, a choline transporter, were. Other genes that have been implicated in AgCC include *Fgfr1, ARX, ZFHX1B, MRPS16,* and *L1CAM* (54), none of which were differently expressed in the transcriptome analysis of the *Tα1tubulin-Cre*/*Ikbkap* CKO in the hindbrain region, but the are including the corpus callosum has not yet been analyzed, so this should be investigated in efforts to determine whether a common genetic expression pattern can be identified in FD and AgCC. Despite an apparent lack of commonality in gene mutation between AgCC and FD, there is commonality of symptoms between the diseases. Furthermore, the etiology of AgCC is variable, and its genetic roots are not well understood.

Individuals with AgCC present with symptoms including hypotonia, scoliosis, delayed walking in childhood (8), visual deficits, decreased pain perception, dysphagia, seizures, and abnormal facial features (9). Because many of the symptoms seen in AgCC are common with those observed in FD patients as well as in the *Tα1tubulin-Cre*/*Ikbkap* CKO mice, the reduction of the corpus callosum in *Ta1tubulin-Cre/Ikbkap* CKO mice remains a potential mechanism for FD symptomology. If the corpus callosum diminution seen in the mouse models of FD translates to human populations as well, this could provide a partial explanation for some of the deficits in FD.

There were no significant differences in the size of the thalamus or in ratio of thalamus to neocortex between mutants and controls. However, the thalamus should be examined in human patients as they do experience a diminution in sensory processing as

a result of *Ikbkap* reduction in the PNS, which may produce observable differences in the thalamus, which serves as a sensory relay station (10).

Though the results of immunohistochemical staining for NPY and NeuN stain did not reach significance due to low numbers of subjects tested (3 control, 3 mutant), the preliminary observations are worth considering. NPY is important in mediating anxiety, and soldiers that have increased levels are more resilient against post traumatic stress disorder and are better able to cope with negative emotion (34). Furthermore, mice whose NPY-Y2 receptors were knocked out, thereby increasing the release of NPY, were less anxious on the elevated plus maze as indicated by the time spent in the open arms (35). These mice also showed better stress coping than controls. Staining for NPY in the mouse CNS should be repeated using more animals, as elevated levels of NPY in the *Tα1tubulin-Cre*/*Ikbkap* CKO mice could help explain their apparent lack of anxiety observed in preliminary testing.

The enhanced brightness of NeuN expression observed in the CA1 region of the *Tα1tubulin-Cre*/*Ikbkap* CKO mouse hippocampus is another observation that did not reach significance due to low subject numbers. Given that the *Tα1tubulin-Cre*/*Ikbkap* CKO mice have lower levels of the Kv1 protein, and thus may have increased neuronal proliferation in the hippocampus, it is possible that there are either more cells in this region, the cells are larger, or they express NeuN more intensely than control cells in the same region. In order to determine whether this observation is significant, the experiment should be repeated on more mice.

While the present study is important in elucidating the role of the central nervous system in FD, it is not without limitation. There was variability in age of mutant-control mouse pairs when they were sacrificed and their brain tissue analyzed. There could have been artifacts produced by the much older tissue compared to that from younger mice. While this is certainly an issue that must be addressed, it is one that is without an apparent solution because there is so much variability in the phenotype and disease severity between affected mice (as well as in human patients), making it impossible to control for age at which the mice become so sick that they must be sacrificed.

Another potential limitation is that the structures were only outlined and measured by one individual. In order to increase reliability of the data, additional researchers should analyze the structures and a measure of inter-user reliability should be calculated. Furthermore, there is variability in the expression of *Cre* within the *Ta1tubulin-Cre/Ikbkap* CKO mice, so phenotypes vary between mutants. This was observed both behaviorally and within brain morphology, where some affected mice appear mostly healthy and others have severe health and CNS deficits and thus die very young. This is problematic when attempting to quantify the extent of damage to brain structures, yet it is also reflective of the true nature of the disease in the human population.

There was variability in the intensity of Nissl staining, as each control-mutant pair was stained at a different time than the other pairs, allowing staining solution to fade between uses. Additionally, some brains took up the stain much more readily than others, producing color variation between animals. Most brain sections were stained well enough

to be able to see all structures of interest, though some had to be discarded due to insufficient staining.

Staining for activated caspase-3, an enzyme responsible for the execution phase of programmed cell death, was attempted, but no conclusive results were found as a result of insufficient staining due either to procedural errors or antibodies that are incompatible with the tissue samples used. This experiment should be repeated in efforts to further analyze whether *Tα1tubulin-Cre*/*Ikbkap* brains have elevated apoptosis. Further, this experiment should be done in embryonic brains to understand whether cell death occurs in utero, or develops in adulthood.

The most obvious limitation of the present study is that it was done on a mouse model of the disease, so while there are certainly commonalities between the symptoms in the *Tα1tubulin-Cre*/*Ikbkap* CKO mice and the human patients, one must be cautious in making conclusions about the deficits underlying the human disease. Furthermore, while the mouse models of FD have *Ikbkap* knocked out only in the CNS, the human FD patients have severe reductions in *Ikbkap* levels in the PNS as well, further limiting the comparability of the mouse model to the human population of interest. Nevertheless, the *Tα1tubulin-Cre*/*Ikbkap* CKO mouse model can provide insight into disease mechanisms in a limited yet significant portion of the nervous system.

Contrasting the results described in the present study, are findings from a neuroimaging study using human FD patients. The study found global atrophy in FD brains compared to controls, where this study found none (26). Furthermore, the human FD brains showed no structural changes in the hippocampus compared to controls, while

the present study found significant increase in hippocampal size compared to controls. This raises concern regarding the level of comparability of findings in the mouse model compared to the human FD population. However, the variability in phenotype of the disease must again be considered, as disease severity varies widely among patients, and the *Tα1tubulin/Cre Ikbkap* mice used in the present study were very sickly. Why global brain atrophy was not observed in these mice remains to be elucidated, but it is possible that the structural changes that were found do not develop until disease severity becomes immense.

This study provides novel evidence for disruption of the central nervous system in a mouse model of familial dysautonomia, and provides support for comorbidity of other disorders that may contribute to the observed deficits in FD patients. Future research should analyze the structures used in the present study in embryonic mice to determine whether each deficit is congenital, progressive, or both.

REFERENCES CITED

1. Axelrod, F.B. (2004) Familial dysautonomia. *Muscle Nerve,* **29**, 352-363.

2. Dietrich, P., Alli, S., Shanmugasundaram, R., and Dragatsis, I. (2012) IKAP expression levels modulate disease severity in a mouse model of Familial Dysautonomia. *Human Molecular Genetics,* 23, 5078-5090.

3. Creppe, C., Malinouskaya, L., Volvert, M., Gillard, M., Close, P., Malaise, O., Laguesse, S., Cornez, I., Rahmouni, S., Ormenese, S., Belachew, S., Malgrange, B., Chapelle, J., Siebenlist, U., Moonen, G., Chariot, A., and Nguyen, L. (2009). Elongator Controls the Migration and Differentiation of Cortical Neurons through Acetylation of α-Tubulin. *Cell,* 136, 551-564.

4. Cornez, I., Creppe, C., Gillard, M., Hennuy, B., Chapelle, J., Dejardin, E., Merville, M., Close P., and Chariot, A. (2008) Deregulated expression of pro-survival and pro-apoptotic p-53-dependent genes upon Elongator deficiency in colon cancer cells. *Biochemical Pharmacology,* 75, 2122-2134.

5. ©2012 Allen Institute for Brain Science. Allen Mouse Brain Atlas [Internet]. Available from: http://mouse.brain-map.org/

6. Rosis, S. (2007). *Synaptic Integration and Plasticity in the Lateral Amygdala.* New York: ProQuest Learning and Information Company.

7. Purves, D., Augustine, G. J., Fitzpatrick, D., Katz, L., LaManta, A., and McNamara, J. O. (1997). *Neuroscience.* Massachusetts: Sinauer Associates Inc.

8. Dupre´, N., Howard, H., Mathieu, J., Karpati, G., Vanasse, M., Bouchard, J., Carpenter, S., and Rouleau, G. (2003). Hereditary Motor and Sensory Neuropathy with Agenesis of the Corpus Callosum. *Annals of Neurology,* 54: 9-18.

9. Doherty, D., Tu, S., Schilmoeller, K., and Schilmoeller, G. (2005). Health-related issues in individuals with agenesis of the corpus callosum. *Child: Care, Health, and Development,* 32: 333-342.

10. Strominger, N.L., Demarest, R.L., and Laemle, L.B. (2005). *Noback's Human Nervous System*, *Seventh Edition: Structure and Function.* New York: Human Press.

11. Axelrod, F.B., and Simson, G.G. (2007). Hereditary sensory and autonomic neuropathies: types II, III, and IV. *Orphanet Journal of Rare Diseases,* 2:39.

12. Siffredi, V., Anderson, V., Leventer, R.J., and Spencer-Smith, M. M. (2013). Neuropsychological Profile of Agenesis of the Corpus Callosum: A Systematic

Review. *Developmental Neuropsychology,* 38: 36-57.

13. Ogino A., Kazui H., Miyoshi N., Hashimoto M., Ohkawa S., Tokunaga H., Ikejiri Y., and Takeda M. (2006). Cognitive Impairment in Patients with Idiopathic Normal Pressure Hydrocephalus. *Dementia and Geriatric Cognitive Disorders.* 12: 113-119.

14. Nestor, S.M., Rupsingh, R., Borrie, M., Smith, M., Accomazzi, V., Wells, J. L., Fogarty, J., and Bartha, R. (2008). Ventricular enlargement as a possible measure of Alzheimer's disease progression validated using the Alzheimer's disease neuroimaging initiative database. *Brain,* 9: 2443-2454.

15. Taylor, M., and David, A.S. (1998). Agenesis of the corpus callosum: a United Kingdom series of 56 cases. *Journal of Neurosurgical Psychiatry,* 64: 131-134.

16. Purves D., Augustine G.J., Fitzpatrick D., Katz, L.C., LaMantia, A., McNamara, J. O., and Williams, S. M. (2001). *Neuroscience, Second Edition.* Massachusetts: Sinauer Associates.

17. Hunnicut, B. J., Chaverra, M., George, L., and Lefcort, F. (2012).Ikap/Elp1 is required in vivo for neurogenesis and neuronal survival, but not for neural crest migration. *PLoS One,* 7: e32050. doi: 10.1371/journal.pone.0032050.

18. Prior, H., Schwegler, H., Marashi, V., and Sachser, N. (2004). Exploration, Emotionality, and Hippocampal Mossy Fibers in Nonaggressive AB/Gat and Congenic Highly Aggressive Mice. *Hippocampus,* 14: 135-140.

19. Schumann, C. M., Hamstra, J., Goodlin-Jones, B.L., Lotspeich, L.J., Kwon, H., Buonocore, M.H., Lammers, C.R., Reiss, A.L., and Amaral, D.G. (2004). The amygdala is enlarged in children but not adolescents with autism; the hippocampus is enlarged at all ages. *The Journal of Neuroscience,* 24: 6392-6401.

20. Kageyama, R., and Yamamori, T. (2013) *Cortical Development: Neural Diversity and Neocortical Organization.* Japan: Springer.

21. Clayton, N.S., and Krebs, J.R. (1994). Hippocampal growth and attrition in birds affected by experience. *Proceedings of the National Acadamy of Sciences of the United States of America,* 91: 7410-7414.

22. Maguire, E.A., Gadian, D.G., Johnsrude, I.S., Good, C.D., Ashburner, J., Frackowiak, R.S.J., and Frith, C.D. (2000). Navigation-related structural change in the hippocampi of taxi drivers. *Proceedings of the National Academy of Sciences of the United States of America,* 97: 4398-4403.

23. Caron, M.J., Mottron, L., Rainville, C., and Chouinard, S. (2004). Do high

functioning persons with autism present superior spatial abilities? *Neuropsychologia,* 42: 467-481.

24. Persson, A., Westman, E., Wang, F., Khan, F.H., Spenger, C., and Lavebratt, C. (2007). Kv1.1 null mice have enlarged hippocampus and ventral cortex. *BMC Neuroscience,* 8: doi:10.1186/1471-2202-8-10.

25. Yellen, G. (2002). The voltage-gated potassium channels and their relatives. *Nature,* 419: 35-42.

26. Axelrod, F.B., Hilz, M.J., Berlin, D., Yau, P.L., Javier, D., Sweat, V., Bruehl, H., and Convit, A. (2010). Neuroimaging supports central pathology in familial dysautonomia. *Journal of Neurology,* 257: 198-206.

27. Axelrod F.B., Zupanc M., Hilz M.J., Kramer, E. L., (2000). Ictal SPECT during autonomic crisis in familial dysautonomia. *Neurology,* 55:122-125.

28. Chen, Y., Hims, M.M., Shetty, R.S., Mull, J., Liu, L., Leyne, M., and Slaugenhaupt, S.A. (2009). Loss of mouse Ikbkap, a subunit of elongator, leads to transcriptional deficits and embryonic lethality that can be rescued by human IKBKAP. *Molecular and Cellular Biology,* 29: 736-744.

29. Mahloudji, M., Brunt, P.W., and McKusick, V.A. (1969). Clinical Neurological Aspects of Familial Dysautonomia. *Journal of the Neurological Sciences,* 11: 383-395.

30. Han, S., Tai, C., Westenbroek, R.E., Yu, F.H., Cheah, C.S., Potter, G.B., Rubernstein, J.L., Scheuer, T., Iglesia, H.O., Catterall, W.A. (2012). Autistic-like behavior in Scn1a$^{+/-}$ mice and rescue by enhanced GABA-mediated neurotransmission. *Nature,* 489: 385-390.

31. Harvey, R. A. , Clark, M. A., Finkel, R., Rey, J. A., Whalen, K. (2012). *Pharmacology, 5th Edition.* Maryland: Lippencott, Williams, and Wilkens.

32. Gabel, L.A. (2011). Layer I neocortical ectopia: cellular organization and local cortical circuitry. *Brain Research,* 1381: 148-158.

33. Boehm, G.W., Sherman, G.F., Rosen, G.D., Galaburda, A.M., and Denenberg, V.H. (1996). Neocortical ectopias in BXSB mice: effects upon reference and working memory systems. *Cerebral Cortex,* 6: 696-700.

34. Yehuda, R., Brand, S., and Yang, R. (2006). Plasma neuropeptide Y concentrations in combat exposed veterans: relationship to trauma exposure, recovery from PTSD, and coping. *Biological Psychiatry,* 59: 660-663.

35. Tschenett, A., Singewald, N., Carli, M., Balducci, C., Salchner, P, Vezzani, A.,

Herzog, H., and Sperk, G. (2003). Reduced anxiety and improved stress coping ability in mice lacking NPY-Y2 receptors. *European Journal of Neuroscience*, 18: 143-148.

36. Janig, W. (2006). *The Integrative Action of the Autonomic Nervous System: Neurobiology of Homeostasis.* New York: Cambridge University Press.

37. Poulin, S.P., Dautoff, R., Morris, J.C., Barrett, L.F., and Dickerson, B.C. (2011). Amygdala atrophy is prominent in early Alzheimer's disease and relates to symptom severity. *Psychiatry Research,* 194: 7-13.

38. Bezchlibnyk, Y.B., Sun, X., Wang, J., MacQueen, G.M., McEwan, B.S., and Young, L.T. (2007). Neuron somal size is decreased in the lateral amygdalar nucleus of subjects with bipolar disorder. *Journal of Psychiatry and Neuroscience*, 32: 203-210.

39. Chang, K., Karchemskiy, A., Barnea-Goraly, N., Garrett, A., Simeonova, D.I., and Reiss, A. (2005). Reduced amygdalar gray matter volume in familial pediatric bipolar disorder. *Journal of the American Acadamy of Child & Adolescent Psychiatry*, 44: 565-573.

40. Parker, S.T., and McKinney, M.L. (1999). *Origins of Intelligence: The Evolution of Cognitive Development in Monkeys, Apes, and Humans*. Maryland: The Johns Hopkins University Press.

41. Yamauchi, H., Fukuyama, H., Nagahama, Y., Katsumi, Y., Dong, Y., Hayashi, T., Konishi, J., and Kimura, J. (1998). Atrophy of the corpus callosum, cortical hypometabolism, and cognitive impairment in corticobasal degeneration. *Archives of Neurology,* 55: 609-614.

42. Rogers, K. (2011). *The Brain and the Nervous System.* New York: Brittanica Educational Publishing.

43. George, L., Chaverra, M., Wolfe, L., Thorne, J., Close-Davis, M., Eibs, A., Riojas, V., Grindeland, A., Orr, M., Carlson, G.A., and Lefcort, F. (2013). Familial Dysautonomia model reveals Ikbkap deletion causes apoptosis of $Pax3^{+}$ progenitors and peripheral neurons. *Proceedings of the National Academy of Science:* doi:10.1073/pnas.1308596110.

44. Pritchard, T.C., and Alloway, K.D. (1992). *Medical Neuroscience.* Connecticut: Fence Creek Publishing.

45. Welton, W., Clayson, D., Axelrod, F.B., Levine, D.B. (1979). Intellectual development and familial dysautonomia. *Pediatrics,* 63:708-12.8.

46. Clark, W.R., and Grunstein, M. (2000). *Are We Hardwired? The Role of Genes in Human Behavior.* New York: Oxford University Press.

47. Gribjoff, V.K., and Kaczmarek, L.K. (2009). *Structure, Function, and Modulation of Neuronal Voltage-gated Ion Channels.* New Jersey: John Wiley & Sons, Inc.

48. Cheischvilli, D., Maayan, C., Smith, Y., Ast, G., and Razin, A. (2007). IKAP/hELP1 deficiency in the cerebrum of familial dysautonomia patients results in down regulation of genes involved in oligodendrocyte differentiation and in myelination. *Human Molecular Genetics,* 16: 2097-2104.

49. Svejstrup, J. (2007). Elongator complex: how many roles does it play? *Current Opinion in Cell Biology,* 19: 331-336.

50. Baer, F., and Hermand, D. (2012). A coordinated codon-dependent regulation of translation by Elongator. *Cell Cycle,* 11: 4524-4529.

51. Karam, D.W. (2012). *Neuroscience: A Medical Student's Guide.* Indiana: Trafford Publishing.

52. Saladin, K. (2009). *Anatomy and Physiology: The Unity of Form and Function.* Georgia: McGraw Hill.

53. Johansen-Berg, H., and Behrens, T.E.J. (2009). *Diffusion MRI: From quantitative measurement to in-vivo neuroanatomy.* California: Elsevier Academic Press.

54. Paul, L. K., Brown, W.S., Adolphs, R., Tyszka, J.M., Richards, L.J., Mukherjee, P., and Sherr, E.H. (2007). Agenesis of the corpus callosum: genetic, developmental and functional aspects of connectivity. *Nature Reviews,* 8: 287-299.

55. Kujawa, K., Babcock, M, and Lefcort, F. (2013). *Familial Dysautonomia: An evaluation of anxiety using the elevated plus maze.* Poster presented at the annual Society for Neuroscience meeting, San Diego, CA.

56. Pritchard, T.C., and Alloway, K.D. (1999). *Medical Neuroscience.* Connecticut: Fence Creek Publishing.